Contrib Mineral Petrol (1982) 80:297–306

Contributions to Mineralogy and Petrology

Petrology of Ultramafic Nodules from West Kettle River, near Kelowna, Southern British Columbia

Toshitsugu Fujii* and Christopher M. Scarfe
Experimental Petrology Laboratory, Department of Geology, University of Alberta, Edmonton, Canada, T6G 2E3

Abstract. A basanitoid flow of Miocene age, exposed near the West Kettle River, 25 km southeast of Kelowna, British Columbia, contains abundant ultramafic and mafic nodules. The subangular nodules are 1–20 cm across and typically show granular textures. A study of 250 nodules indicates that spinel lherzolite (~60%) is the dominant type with subordinate olivine websterite (~10%), websterite (~7%), clinopyroxenite (~4%), wehrlite (~4%), pyroxene gabbro (~4%), dunite (~2%), harzburgite (~1%) and granitic rocks (~8%). Ultramafic nodules are of two types. Most of the wehrlites and clinopyroxenites belong to the black pyroxene (aluminous clinopyroxene) series, whereas the other clinopyroxene-bearing nodules belong to the green pyroxene (chromian diopside) series. Some spinel lherzolite nodules have distinctive pyroxene- and olivine-rich bands. Microprobe analyses of the constituent minerals of more than thirty nodules from the green pyroxene series indicate that grain to grain variations within individual nodules are small even when banding is present. Olivine, orthopyroxene, clinopyroxene and spinel in spinel lherzolite have average compositions of Fo_{90}, En_{90}, $Wo_{47}Fs_5En_{48}$, $Cr/(Cr+Al+Fe^3)=0.1$ and $Mg/(Mg+Fe^{2+})=0.8$. Equilibration temperatures, which were calculated using the two pyroxene geothermometer of Wells (1977), range between 920–980° C. Based on published phase stability experiments, pressures of equilibration are between 10–18 kbar. In summary, the upper mantle beneath southern British Columbia is dominated by spinel lherzolite but contains some banding on a scale of cm to meters. The temperature in the upper mantle is ~950° C at a depth of 30–60 km.

Introduction

The study of mantle nodules transported to the surface by alkali basalts has been an important area of research for several years (e.g. Kuno and Aoki 1970; Jackson and Wright 1970; Yoder 1976). Only a few nodule localities, however, have been described in British Columbia (e.g. Littlejohn and Greenwood 1974; Fiesinger and Nicholls 1977; Hamilton 1981; Nicholls et al. 1982) where Late Tertiary to Recent volcanism is represented by a large component of alkali basalts (Souther 1970; 1977).

In this paper we describe a suite of approximately 200 nodules from a Miocene lava flow exposed in the West Kettle River valley, 25 km southeast of Kelowna, British Columbia. Nodules from this locality have not been previously described. We present petrographic, textural, mineralogical and chemical data on the nodules and derive temperatures of equilibration using element partition geothermometers. Using these temperatures, and estimates for the depth of origin of the nodules, we discuss the geothermal gradient and the nature of the upper mantle beneath southern British Columbia.

Geological Setting and Host Basalts

The host basalts are part of a northwest-trending belt of Late Cenozoic volcanism in British Columbia (Souther 1970; Nicholls et al. 1982). Four lava flows are exposed on a forestry road to the west of the West Kettle River valley in the Kettle River Provincial Forest (geological map sheet 82E (west half); 49°47′N, 119°4′W; Fig. 1). Their age has not been determined radiometrically, but according to the geological relationships they are most probably of Miocene age (Hamilton, personal communication). The four flows are stacked concordantly and have thicknesses of approximately 2 m, except for the nodule-bearing flow which is 11 m thick. Each flow is separated by a rubbly horizon about 10 cm thick; however, no weathering surfaces were detected, suggesting that the flows were erupted without a significant time lag. Only the uppermost flow is nodule-bearing and it also shows well developed columnar joints with 50 cm average widths of columns. The uppermost flow can be seen in contact with the gneissic basement at the west end of the section.

The host basalt has phenocrysts of olivine (~10%) and rarely clinopyroxene (~2%) within an intergranular groundmass of plagioclase, clinopyroxene, olivine and titanomagnetite. Olivine phenocrysts are mostly euhedral and free from alteration. Clinopyroxene phenocrysts occur as both euhedral and anhedral crystals, often showing good examples of sector zoning. Groundmass olivine is subhedral and commonly associated with euhedral or subhedral titanomagnetite. Groundmass clinopyroxenes are mostly granular and relatively rare columnar structures are found in feldspar-rich portions of the groundmass. The columnar pyroxene shows sector zoning of the swallowtail type (Strong 1969).

Xenocrysts of olivine, orthopyroxene and clinopyroxene, thought to be derived from disaggregated ultramafic

* On leave from the Geological Institute, University of Tokyo, Japan

Reprint requests to: C.M. Scarfe

0010-7999/82/0080/297/$02.00

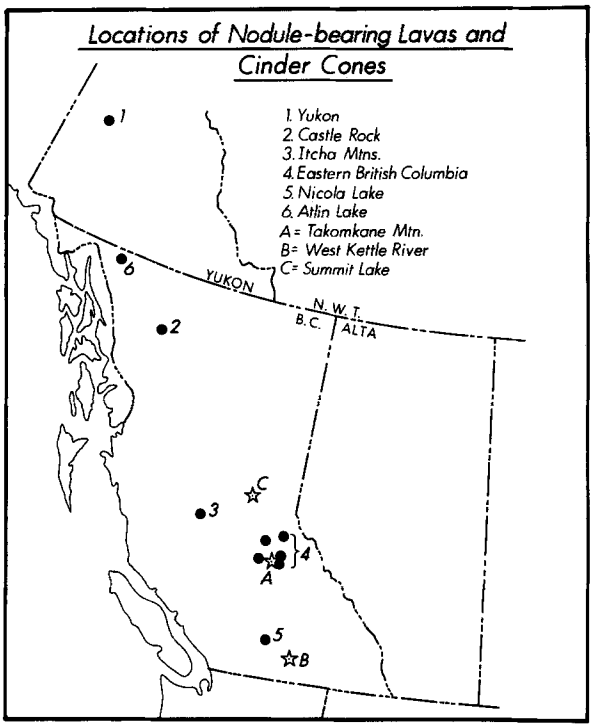

Fig. 1. Locations of nodule-bearing lavas and cinder-cones of Late Cenozoic age in Western Canada. (*1*) Sinclair et al. 1978; (*2, 4* and *5*) Littlejohn and Greenwood 1974; (*3* and *6*) Nicholls et al. (1972); (*A*) Fujii and Scarfe 1981; (*B*) Fujii et al. 1981; (*C*) Brearley et al. (1982)

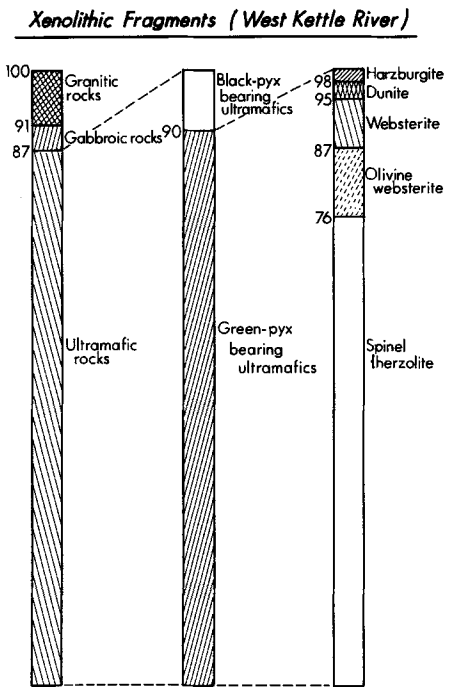

Fig. 2. Percentages of types of xenolithic fragments at West Kettle River. Estimates from 250 nodules in the field

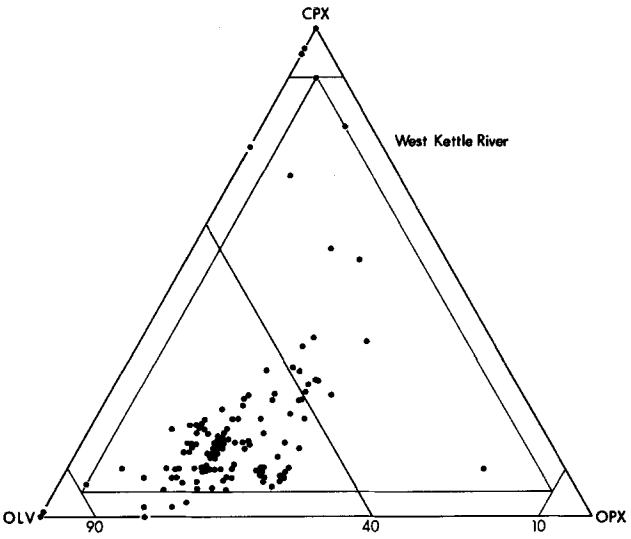

Fig. 3. Modal mineralogy of green pyroxene series nodules plotted in terms of olivine, orthopyroxene and clinopyroxene. Laboratory estimates of 100 nodules

nodules, are also present. The xenocrysts frequently show evidence of reaction with the magma. Xenocrystic olivine shows irregular grain surfaces and xenocrysts of orthopyroxene have ragged crystal outlines and are surrounded by aggregates of small olivine grains that are probably the product of reaction with the host basaltic liquid. Xenocrystic clinopyroxene occurs as rounded crystals surrounded by a rim of titanaugite. Dusty inclusions mark the boundary between the two phases.

Ultramafic Nodules

Xenolithic fragments are concentrated in the lower middle portion of the uppermost basalt flow and occupy about 0.5 volume percent of the flow. The xenoliths are mostly subangular and range from 1–20 cm in diameter, with an average size of about 5 cm. They range from gneissic rocks of crustal origin to ultramafic rocks of upper mantle origin. The frequency of each type (Fig. 2) was estimated from the field observation of about 250 xenoliths in one outcrop which was approximately 11 m high and 75 m in length.

The textures of the ultramafic nodules are typically granular with average grain sizes of 1–2 mm. They can be subdivided into two series: a dominant green-pyroxene and a subordinate black-pyroxene series (Wilshire and Shervais 1975). The black-pyroxene series rocks contain abundant clinopyroxene and lesser amounts of olivine and are classified as olivine-clinopyroxenite and clinopyroxenite. On the other hand, rocks of the green pyroxene series have abundant olivine, orthopyroxene, clinopyroxene and small amounts of spinel. They are mainly lherzolite and olivine websterite; however, there are a few samples of harzburgite and dunite. The modal proportions of the green-pyroxene series rocks are shown in Fig. 3 in terms of olivine, orthopyroxene and clinopyroxene. Some of the lherzolites have bands enriched in clinopyroxene or orthopyroxene (Fig. 4). The thicknesses of the bands vary from 0.5 cm to several cm, and it is possible that some of the olivine websterite plotted in Fig. 3 represents fragments of the pyroxene-enriched bands.

No significant reaction zones between the xenoliths and the host basalt were recognized, except in the case of gabbroic or gneissic samples of crustal origin. In some ultramafic nodules of the green pyroxene series, however, partial melting along grain boundaries was observed. It is suggested below that this melting took place after capture of the fragments by the host basalt.

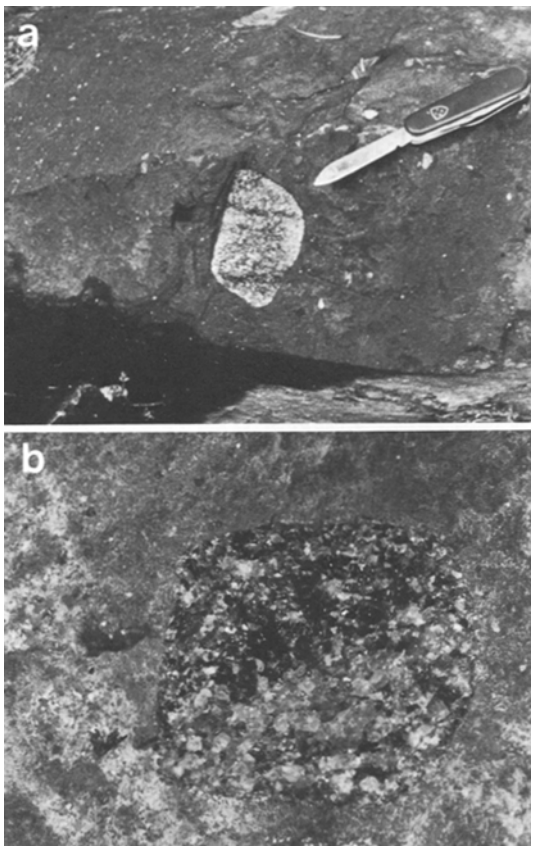

Fig. 4. Examples of banding in nodules. **a** Nodule showing dark bands rich in chrome diopside. Width of nodule ~6 cm. **b** Nodule divided into two halves, one rich in chrome diopside, the other rich in olivine. Width of nodule ~3 cm

Analytical Methods

Chemical analyses of phases in nodules of the green pyroxene series and the host basalt were performed on an ARL EMX microprobe fitted with an Ortec energy-dispersive spectometer. Operating conditions were 15 kV operating voltage, 20 nA probe current and 400 s counting times at a full-spectrum counting rate of approximately 3,000/s. The spectra were processed by using EDATA2 (Smith and Gold 1979). The limit of detection using the above methods is ~500 ppm and accuracies for major and minor elements are comparable to wavelength dispersive analysis (Smith 1976; Smith and Gold 1979).

A few analyses were also performed on the MAC wavelength dispersive microprobe at the Geophysical Laboratory, Carnegie Institution of Washington. Data reduction for the MAC microprobe was performed by the methods of Bence and Albee (1968). The results obtained by the two different methods are identical within analytical error.

Analyses of the host basalt were performed by microprobe on glass beads fused from basalt powder at about 1,350° C in air. FeO was determined wet chemically by a volumetric titration method (Wilson 1960).

Bulk Chemistry and Mineral Chemistry of the Host Basalt

The chemical composition and CIPW norm of the host basalt is given in Table 1. The rock has no modal nepheline but contains 12.3% nepheline in the norm and is classified as a basanitoid (Macdonald and Katsura 1964).

Table 1. Chemical composition of the host basalt

SiO_2	44.5
TiO_2	3.12
Al_2O_3	14.1
Cr_2O_3	0.08
Fe_2O_3	3.73
FeO	8.52
MnO	0.21
MgO	9.50
CaO	9.55
Na_2O	4.20
K_2O	1.65
P_2O_5	0.79
Total	99.95
CIPW norm	
or	9.75
ab	12.92
an	14.75
ne	12.25
di-wo	11.47
di-en	7.92
di-fs	2.61
fo	11.03
fa	4.01
mt	5.41
il	5.93
ap	1.83

Representative compositions of phenocryst and groundmass phases are shown in Table 2. The core compositions of olivine phenocrysts (Fo_{84}, CaO = 0.2 wt.%) are relatively homogeneous and are mantled by a narrow (< 50 μm) strongly-zoned rim. Rim compositions vary towards the perimeter from $Fo_{83}-Fo_{69}$ with CaO contents ranging from 0.2–0.6 wt.%, and the composition of the outermost zone is similar to the composition of groundmass olivine. Clinopyroxene phenocrysts are titanaugites with distinct differences in core and rim compositions. Xenocrysts of olivine (Fo_{91}) and orthopyroxene (En_{90}) are also present.

Groundmass olivine is ~Fo_{69} and plagioclase in the groundmass is typically zoned from An_{61} to An_{52}. Groundmass clinopyroxene is titanaugite, but it is much less aluminous than the phenocryst clinopyroxene. Titanomagnetite shows a slight increase in the ulvöspinel component and a decrease in MgO and Al_2O_3 (3.7 to 2.8 wt.% MgO; 4.4 to 2.5 wt.% Al_2O_3) towards the margin. The petrogenesis of the basalts will be discussed elsewhere (Scarfe and Fujii, in preparation).

Mineral Chemistry of the Nodules

Microprobe analyses of the constituent minerals of 35 nodules from the green pyroxene series are described below. Representative analyses are given in Tables 3 and 4. Analyses of the black pyroxene series xenoliths and of the crustal samples are not discussed in this paper.

Olivine. Olivine varies in composition from $Fo_{87}-Fo_{92}$, but is mostly within the range $Fo_{89}-Fo_{91}$ (see data plotted in Fig. 7 in next section). The content of NiO varies from

Table 2. Chemical Composition of Minerals in the host basalt (KR-119)

	OLV 2-1* (Ph-core)	OLV 2-7 (Ph-rim)	OLV 3-2 (Gm)	CPX 1-1 (Ph-core)	CPX 1-4 (Ph-rim)	CPX 4-1 (Gm)	PLG 2-1 (Mph)	PLG 4-2 (Gm)	MT 1-1 (Mph)	MT 6-1 (Gm)
SiO_2	39.1	38.0	37.0	47.3	43.3	46.9	52.4	54.3	n.d.	0.15
TiO_2	n.d.	0.06	0.08	1.98	4.22	2.68	0.09	0.15	20.9	22.3
Al_2O_3	n.d.	0.06	n.d.	9.41	9.13	6.02	29.1	28.4	4.42	2.56
Cr_2O_3	n.d.	n.d.	n.d.	0.14	0.07	n.d.	n.d.	n.d.	0.47	0.13
Fe_2O_3	n.a.	n.a.	n.a.	n.a.	n.a.	n.a.	n.a.	n.a.	20.0	19.4
FeO	15.4	22.8	27.8	7.43	8.12	7.75	0.47	0.56	48.6	50.8
MnO	0.11	0.39	0.60	0.18	0.11	0.16	0.07	n.d.	0.69	0.78
MgO	44.0	38.1	34.0	13.4	11.3	12.7	0.11	0.11	3.71	2.90
CaO	0.21	0.36	0.53	18.3	22.1	22.2	12.1	10.9	0.13	0.17
Na_2O	n.d.	n.d.	n.d.	0.79	0.37	0.48	4.02	4.67	n.d.	n.d.
K_2O	n.d.	n.d.	n.d.	n.d.	n.d.	n.d.	0.30	0.34	n.d.	n.d.
NiO	0.21	n.d.	n.d.	n.d.	n.d.	0.06	n.d.	n.d.	n.d.	n.d.
Total	99.03	99.77	100.01	98.93	98.72	98.95	98.66	99.43	98.92	99.19
O	4.000	4.000	4.000	6.000	6.000	6.000	8.000	8.000	4.000	4.000
Si	0.995	0.995	0.993	1.762	1.656	1.777	2.409	2.467	n.d.	0.006
Al	n.d.	0.002	n.d.	0.413	0.411	0.269	1.576	1.521	0.191	0.112
Ti	n.d.	0.001	0.002	0.055	0.121	0.076	0.003	0.005	0.575	0.621
Cr	n.d.	n.d.	n.d.	0.004	0.002	n.d.	n.d.	n.d.	0.014	0.004
Fe^{3+}	n.a.	n.a.	n.a.	n.a.	n.a.	n.a.	n.a.	n.a.	0.550	0.539
Fe^{2+}	0.328	0.499	0.624	0.231	0.260	0.246	0.018	0.021	1.489	1.573
Mn	0.002	0.009	0.014	0.006	0.004	0.005	0.003	n.d.	0.021	0.024
Mg	1.669	1.487	1.359	0.744	0.644	0.717	0.008	0.007	0.202	0.160
Ca	0.006	0.010	0.015	0.730	0.905	0.901	0.596	0.531	0.005	0.007
Na	n.d.	n.d.	n.d.	0.057	0.027	0.035	0.358	0.411	n.d.	n.d.
K	n.d.	n.d.	n.d.	n.d.	n.d.	n.d.	0.018	0.020	n.d.	n.d.
Ni	0.004	n.d.	n.d.	n.d.	n.d.	0.002	n.d.	n.d.	n.d.	n.d.
Total	3.005	3.003	3.006	4.003	4.030	4.029	4.988	4.983	3.048	3.046
Mg/Mg+Fe	83.6	74.9	68.6	76.3	71.3	74.5	–	–	–	–
Ca	0.3	0.5	0.8	42.8	50.1	48.4	–	–	–	–
Mg	83.4	74.5	68.0	43.6	35.6	38.5	–	–	–	–
Fe	16.4	25.0	31.2	13.6	14.4	13.2	–	–	–	–

Ph: phenocryst; Gm: groundmass; Mph: microphenocryst; n.a.: not analyzed; n.d.: not detected

* Laboratory analysis number

0.4–0.5 wt.% and shows no systematic relationship with forsterite content. The concentration of CaO is close to the detection limit of the microprobe. Detailed profiling of grains yielded no chemical zonation of MgO, FeO, NiO and CaO and grain-to-grain heterogeneities within single nodules are absent. Even in banded lherzolites, olivines in olivine-rich bands are identical in composition to those in pyroxene-rich bands.

Orthopyroxene. Orthopyroxene compositions range from $Ca_1Mg_{91}Fe_8$ to $Ca_1Mg_{88}Fe_{11}$ (Fig. 5). The Al_2O_3 content is between 2–5 wt.% and the Cr_2O_3 content is less than 0.6 wt.%. Within a given nodule, the composition of orthopyroxene is homogeneous and exsolution phases were not found. With decreasing Mg/(Mg+Fe), Al_2O_3 increases and Cr_2O_3 decreases. Furthermore, Al_2O_3 decreases systematically as the Cr/(Cr+Al) values in coexisting spinel increase (Fig. 6a).

Clinopyroxene. Most clinopyroxenes have compositions within a narrow region around $Ca_{47}Mg_{48}Fe_5$ (Fig. 5). Within individual nodules there is little or no compositional heterogeneity in CaO, MgO, FeO, Al_2O_3 and Cr_2O_3. Some grains in a few nodules have exsolution lamellae of orthopyroxene. No compositional differences, however, could be detected between these grains and exsolution-free grains. There is some nodule to nodule variation in Al_2O_3 (3–8 wt.%) and Cr_2O_3 (0.6–1.6 wt.%). These two elements show good correlation when the Al_2O_3 content of clinopyroxene is plotted against Cr/(Cr+Al) in coexisting spinels (Fig. 6b).

Spinel. The major variation in the chemical composition of spinels is in the ratio of $Cr/(Cr+Al+Fe^{3+})=0.06$–0.5 and in $Mg/(Mg+Fe^{2+})=0.84$–0.7, with most values clustering around 0.1 and 0.82, respectively. This is somewhat unusual, because spinels in ultramafic nodules are often heterogeneous within individual nodules, even when the silicate minerals are homogeneous (e.g. Wilshire and Jackson 1975). The range of spinel compositions for a nodule, KR-92, are given in Table 4. Compositional zoning at grain boundaries could not be detected.

Estimation of Equilibration Temperatures

Because of the homogeneity of mineral compositions in individual nodules at West Kettle River, it is reasonable to assume that the minerals within a given nodule are well

Table 3. Representative analyses of minerals in ultramafic nodules

	1 OLV 1-1	2 CPX 1-1	3 OLV 1-1	4 OPX 1-1	5 CPX 1-1	6 SPN 1-1	7 OLV 1-1	8 OPX 1-1	9 CPX 1-1	10 SPN 1-1	11 OLV 1-1
SiO_2	40.4	52.9	40.9	54.8	52.7	0.37	40.2	55.3	52.1	n.d.	40.2
TiO_2	n.d.	0.18	n.d.	n.d.	0.19	n.d.	n.d.	n.d.	0.46	0.14	n.d.
Al_2O_3	n.d.	4.57	n.d.	4.17	5.79	55.9	n.d.	3.92	6.59	55.3	n.d.
Cr_2O_3	n.d.	1.64	n.d.	0.36	0.96	11.5	n.d.	0.35	1.10	12.5	n.d.
Fe_2O_3	n.a.	n.a.	n.a.	n.a.	n.a.	2.93	n.a.	n.a.	n.a.	2.26	n.a.
FeO	8.23	1.99	9.42	5.97	2.49	7.22	9.62	6.09	2.63	8.47	10.5
MnO	0.10	n.d.	0.12	0.11	n.d.	0.07	0.12	0.13	n.d.	n.d.	0.14
MgO	50.5	15.6	49.5	33.5	15.5	21.5	49.6	33.6	15.0	20.9	48.9
CaO	n.d.	21.1	n.d.	0.53	20.9	n.d.	n.d.	0.56	19.9	n.d.	n.d.
Na_2O	n.d.	1.39	n.d.	n.d.	1.25	n.d.	n.d.	n.d.	1.58	n.d.	n.d.
NiO	0.49	n.d.	0.38	0.08	0.09	0.37	0.40	n.d.	n.d.	0.44	0.38
Total	99.72	99.37	100.32	99.52	99.87	100.06	99.94	99.95	99.36	100.01	100.12
O	4.000	6.000	4.000	6.000	6.000	4.000	4.000	6.000	6.000	4.000	4.000
Si	0.989	1.924	0.998	1.900	1.906	0.010	0.988	1.909	1.892	n.d.	0.990
Al	n.d.	0.196	n.d.	0.170	0.247	1.699	n.d.	0.159	0.282	1.694	n.d.
Ti	n.d.	0.005	n.d.	n.d.	0.005	n.d.	n.d.	n.d.	0.013	0.003	n.d.
Cr	n.d.	0.047	n.d.	0.010	0.027	0.234	n.d.	0.010	0.032	0.257	n.d.
Fe^{3+}	n.d.	n.d.	n.d.	n.d.	n.d.	0.057	n.d.	n.d.	n.a.	0.044	n.a.
Fe^{2+}	0.168	0.061	0.192	0.173	0.075	0.156	0.198	0.176	0.080	0.184	0.216
Mn	0.002	n.d.	0.002	0.003	n.d.	0.002	0.002	0.004	n.d.	n.d.	0.003
Mg	1.842	0.846	1.801	1.731	0.835	0.827	1.816	1.729	0.812	0.810	1.794
Ca	n.d.	0.822	n.d.	0.020	0.810	n.d.	n.d.	0.021	0.774	n.d.	n.d.
Na	n.d.	0.98	n.d.	n.d.	0.088	n.d.	n.d.	n.d.	0.111	n.d.	n.d.
Ni	0.010	n.d.	0.007	0.002	0.003	0.008	0.008	n.d.	n.d.	0.009	0.008
Total	3.011	3.998	3.002	4.010	3.996	2.995	3.012	4.007	3.995	3.000	3.010
Mg/Mg+Fe	91.6	93.3	90.4	90.9	91.7	84.1	90.2	90.8	91.0	81.5	89.3
Ca(Al)	0.0	47.6	0.0	1.0	47.1	85.4	0.0	1.1	46.5	84.9	0.0
Mg(Cr)	91.6	48.9	90.4	90.0	48.6	11.8	90.2	89.8	48.7	12.9	89.3
Fe(Fe^{3+})	8.4	3.5	9.6	9.0	4.4	2.9	9.8	9.1	4.8	2.2	10.8

	12 OPX 1-1	13 CPX 1-1	14 OLV 1-1	15 OLV 1-1	16 OPX 1-1	17 CPX 1-1	18 SPN1-1	19 OLV 1-1	20 OPX 1-1	21 CPX 1-1	22 SPN 1-1
SiO_2	54.6	51.4	39.7	39.9	54.4	51.8	0.11	39.8	55.2	52.5	n.d.
TiO_2	n.d.	0.65	n.d.	n.d.	0.12	0.57	n.d.	n.d.	n.d.	0.20	0.71
Al_2O_3	4.51	7.27	n.d.	n.d.	4.52	7.75	60.8	n.d.	3.23	4.99	37.2
Cr_2O_3	0.27	0.83	n.d.	n.d.	0.22	0.81	6.43	n.d.	0.40	1.26	26.4
Fe_2O_3	n.a.	n.a.	n.a.	n.a.	n.a.	n.a.	2.37	n.a.	n.a.	n.a.	6.24
FeO	6.64	2.77	10.4	10.5	6.76	2.86	8.27	12.0	7.43	3.56	12.4
MnO	0.16	0.07	0.15	0.08	0.17	n.d.	n.d.	0.19	0.15	0.07	n.d.
MgO	32.5	14.6	48.3	48.2	32.4	14.6	21.4	47.6	32.7	16.1	16.9
CaO	0.57	19.8	n.d.	0.09	0.58	19.8	n.d.	n.d.	0.70	19.6	n.d.
Na_2O	n.d	1.80	n.d.	n.d.	n.d.	1.63	n.d.	n.d.	n.d.	1.36	n.d.
NiO	n.d.	n.d.	0.46	0.47	0.11	n.d.	0.56	0.37	n.d.	n.d.	0.36
Total	99.25	99.19	99.01	99.24	99.28	99.82	99.94	99.96	99.81	99.64	100.19
O	6.000	6.000	4.000	4.000	6.000	6.000	4.00	4.000	6.000	6.000	4.000
Si	1.902	1.872	0.989	0.992	1.897	1.872	0.003	0.989	1.920	1.910	n.d.
Al	0.185	0.312	n.d.	n.d.	0.186	0.330	1.823	n.d.	0.132	0.214	1.242
Ti	n.d.	0.018	n.d.	n.d.	0.003	0.015	n.d.	n.d.	n.d.	0.005	0.015
Cr	0.007	0.024	n.d.	n.d.	0.006	0.023	0.129	n.d.	0.011	0.036	0.591
Fe^{3+}	n.a.	n.a.	n.a.	n.a.	n.a.	n.a.	0.045	n.a.	n.a.	n.a.	0.133
Fe^{2+}	0.193	0.084	0.217	0.218	0.197	0.086	0.176	0.249	0.216	0.108	0.293
Mn	0.005	0.002	0.003	0.002	0.005	n.d.	n.d.	0.004	0.004	0.002	n.d.
Mg	1.687	0.793	1.793	1.785	1.684	0.786	0.811	1.762	1.695	0.873	0.714
Ca	0.021	0.773	n.d.	0.002	0.022	0.766	n.d.	n.d.	0.026	0.764	n.d.
Na	n.d.	0.127	n.d.	n.d.	n.d.	0.114	n.d.	n.d.	n.d.	0.096	n.d.
Ni	n.d.	n.d.	0.009	0.009	0.003	n.d.	0.011	0.007	n.d.	n.d.	0.008
Total	4.002	4.005	3.011	3.008	4.004	3.993	2.999	3.011	4.006	4.008	2.997
Mg/Mg+Fe	89.7	90.4	89.2	89.1	89.5	90.1	82.2	87.6	88.7	89.0	70.9
Ca(Al)	1.1	46.8	0.0	0.1	1.1	46.8	91.3	0.0	1.4	43.8	63.2
Mg(Cr)	88.7	48.1	89.2	89.0	88.5	48.0	6.5	87.6	87.5	50.0	30.1
Fe(Fe^{3+})	10.2	5.1	10.8	10.9	10.4	5.3	2.3	12.4	11.1	6.2	6.8

1-2, KR-106 wehrlite; 3-6, KR-1 lherzolite; KR-5 lherzolite; 11-13, KR-46A lherzolite; 14-17, KR-46B olivine websterite; 18-21, KR-61 lherzolite

Table 4. Chemical composition of spinel in a spinel lherzolite (KR-92)

	SPN 1-1	SPN 2-B	SPN 2-1	SPN 2-2	SPN 2-3	SPN 2-4	SPN 2-5	SPN 3-1
SiO_2	0.15	0.09	0.10	0.10	0.10	0.11	0.06	n.d.
TiO_2	0.15	0.13	0.15	0.15	0.15	0.13	0.13	0.12
Al_2O_3	58.5	58.1	59.0	58.8	57.3	57.7	57.9	58.8
Cr_2O_3	7.63	7.73	7.24	8.01	8.12	7.96	7.71	7.92
Fe_2O_3	3.87	3.31	2.18	2.68	3.78	3.32	4.03	3.11
FeO	7.72	8.02	8.94	8.79	7.60	8.01	7.38	8.30
MnO	n.d.	0.11	0.12	0.09	n.d.	0.12	0.16	n.d.
MgO	21.7	21.2	20.7	21.0	21.4	21.1	21.6	21.4
NiO	0.46	0.42	0.31	0.40	0.46	0.43	0.47	0.36
Total	100.18	99.11	98.74	100.02	98.91	98.88	99.43	100.01
O	4.000	4.000	4.000	4.000	4.000	4.000	4.000	4.000
Si	0.004	0.002	0.003	0.003	0.003	0.003	0.002	n.d.
Al	1.762	1.770	1.801	1.778	1.751	1.764	1.758	1.775
Ti	0.003	0.003	0.003	0.003	0.003	0.003	0.003	0.002
Cr	0.154	0.158	0.148	0.162	0.166	0.163	0.157	0.160
Fe^{3+}	0.074	0.064	0.043	0.052	0.074	0.065	0.078	0.060
Fe^{2+}	0.165	0.173	0.194	0.189	0.165	0.174	0.159	0.178
Mn	n.d.	0.002	0.003	0.002	n.d.	0.003	0.003	n.d.
Mg	0.827	0.817	0.799	0.803	0.827	0.816	0.830	0.817
Ni	0.009	0.009	0.006	0.008	0.010	0.009	0.010	0.007
Total	2.998	2.999	2.999	2.999	2.999	2.999	2.999	3.000
$Mg/Mg+Fe^{2+}$	83.4	82.5	80.5	81.0	83.4	82.4	83.9	82.1
Al	88.3	88.8	90.3	89.2	87.8	88.6	88.3	88.9
Cr	7.7	7.9	7.4	8.1	8.4	8.2	7.9	8.0
Fe^{3+}	3.9	3.2	2.2	2.6	3.8	3.2	3.8	3.1

Fe^{2+}: Fe^{3+} determined by stoichiometry; n.d.: not detected

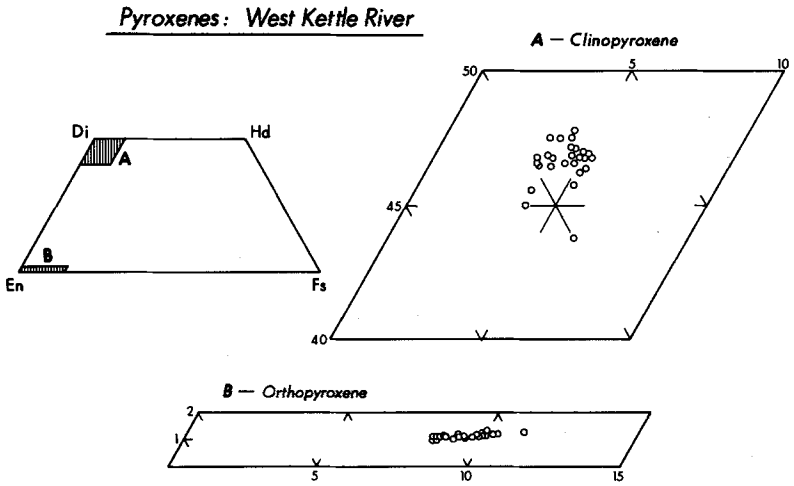

Fig. 5. Compositional plots of pyroxenes in nodules from West Kettle River

equilibrated. It is therefore possible to calculate temperatures of equilibration using published geothermometers. Unfortunately, few published geothermometers are reliable.

The partitioning of Fe and Mg between olivine and clinopyroxene is temperature dependent. This geothermometer, however, has not been calibrated experimentally and there have been problems with the theoretical treatment (Powell and Powell 1974; Mori and Green 1978). Wood (1976) discussed some of the shortcomings in a commentary on the paper of Powell and Powell (1974). Nevertheless, a qualitative estimate of the equilibration temperatures can be obtained by using Fe-Mg partitioning, especially in the case of equilibration at low temperatures. In Fig. 7, Mg/(Mg+Fe) ratios of coexisting olivine and clinopyroxene are shown. All points for the West Kettle River nodules plot between the line for $K=1$ and the line for coexisting olivine and clinopyroxene in Norwegian granulites. The latter is believed to correspond to equilibration temperatures of 700–750° C (Mori and Banno 1973; Obata et al. 1974). Igneous rocks scatter around the line $K=1$ (Obata et al. 1974). Equilibration temperatures for the West Kettle River nodules are therefore between 750° C and igneous temperatures of 1,200° C. This temperature range is lower than the liquidus temperature of anhydrous basalts at pressures greater than 10 kbar (Yoder 1976).

The two-pyroxene geothermometer, which is based on

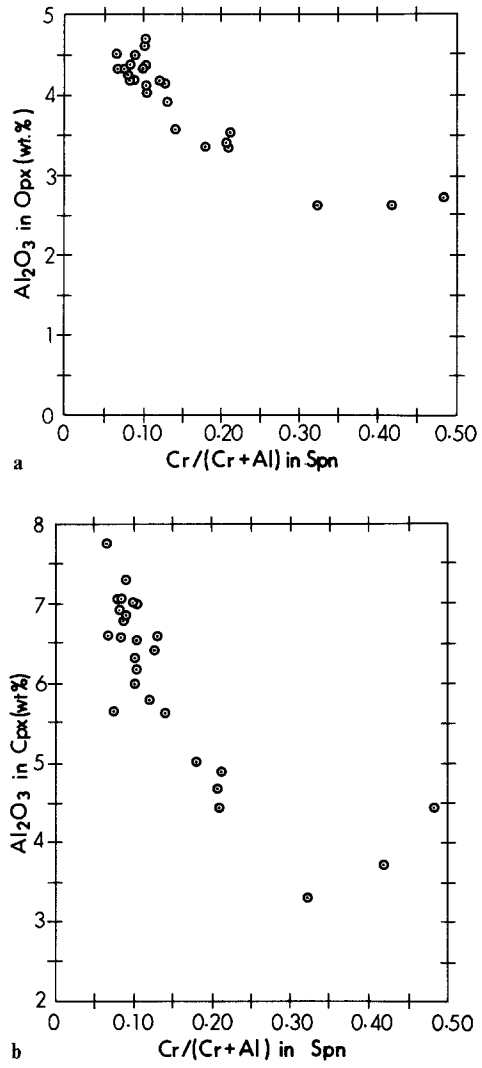

Fig. 6. Plots of Al_2O_3 in orthopyroxenes (**a**) and clinopyroxenes (**b**) against Cr/(Cr+Al) in spinels

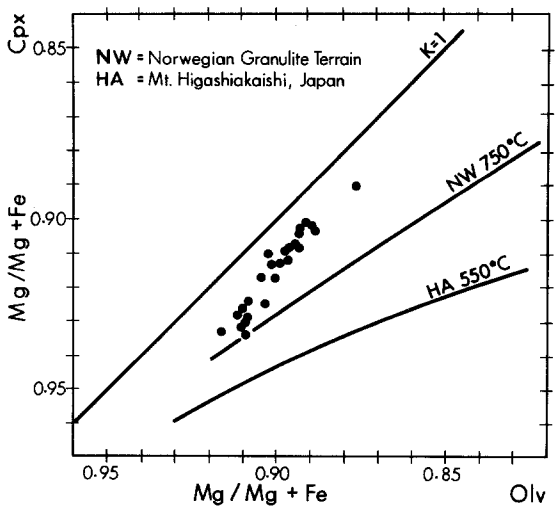

Fig. 7. Mg/(Mg+Fe) ratios of coexisting olivine and clinopyroxene in nodules from West Kettle River

the width of the miscibility gap between orthopyroxene and clinopyroxene, has frequently been used to estimate the equilibration temperatures of ultramafic rocks. However, as pointed out by Henry and Medaris (1980), temperatures estimated with different formulations of the two-pyroxene geothermometer give conflicting results. Despite these reservations, and even though there seems to be no consensus on which two-pyroxene geothermometer is most adequate, the geothermometer of Wells (1977) is commonly used. We have therefore applied the Wells' two-pyroxene geothermometer to the West Kettle River nodules. Twenty-five of the nodules which contain two pyroxenes were equilibrated in a narrow temperature range from 920–980° C, and the remaining five nodules extend this range from 900–1,040° C. The uncertainties inherent in the geothermometer are less than $\pm 50°$ C and those derived from the probe data are less than $\pm 10°$ C for each calculated temperature. If, on the other hand, Wood and Banno's (1973) two-pyroxene geothermometer is applied, all temperatures are systematically about 100° C higher than those of Wells.

Other methods based on the solubility of elements, such as aluminum solubility in orthopyroxene (MacGregor 1974), have not been generally successful. Henry and Medaris (1980) applied several methods to ultramafic rocks found in ophiolites and concluded that the method of aluminum solubility in orthopyroxene (Fuji 1976; Danckwerth and Newton 1978) can be used successfully because 'temperature estimates can be made from the composition of orthopyroxene alone, rather than from the compositions of coexisting orthopyroxene, spinel and olivine' and 'even in disequilibrium situations orthopyroxene compositions may yield reliable temperatures provided that orthopyroxene was at one time in equilibrium with olivine and spinel'. In fact, this is incorrect. As discussed by Fujii (1976) and Danckwerth and Newton (1978), the solubility of aluminum in orthopyroxene is a function not only of temperature and pressure, but also of the composition of coexisting olivine and spinel. Although the equations proposed by Fujii (1976) and Danckwerth and Newton (1978) include ideal solution corrections allowing for additional components in pyroxene and spinels, their applicability in multicomponent systems, especially the Cr-bearing system, has not yet been tested experimentally. A recent study (Sachtleben and Seck 1981) indicates that the ideal solution correction for spinel is not adequate and that the Cr/Cr+Al ratio in spinel has a significant effect on the geothermometer. The application of this geothermometer to the West Kettle River nodules gave consistent results for Cr-poor assemblages but inconsistent results for Cr-rich assemblages.

The olivine-spinel geothermometer, which depends on the partitioning of iron and magnesium between coexisting olivine and spinel, also has several contradictory versions (Jackson 1969; Evans and Frost 1975; Fujii 1977; Fabriès 1979; Roeder et al. 1979). One of the reasons for disagreement is the difficulty of carrying out successful calibration experiments at low temperatures. The early version of this geothermometer was calibrated at high temperatures with data from olivine-spinel assemblages in natural basalt (Evans and Frost 1975). These calibrations, however, are less reliable than laboratory experiments, because it is not clear that coexisting olivine and spinel actually crystallized at liquidus temperatures in equilibrium with each other. Furthermore, because spinels in spinel lherzolite are often

very aluminous and the effect of temperature on the Fe-Mg partition coefficient is too sensitive for such spinels (Fujii 1977; Fabriès 1979), small analytical errors can cause large changes in estimated temperatures.

Estimation of Equilibration Pressures

There are no reliable geobarometers for spinel lherzolite. The only way to estimate the depth of equilibration is from the published phase relationships for spinel lherzolite. A maximum pressure of 19 kbar at 1,100° C is indicated by the absence of garnet (Obata 1976; Herzberg 1978) and a minimum pressure of 10 kbar at 1,100° C is defined by the absence of plagioclase. The rather small variations in equilibration temperature suggest that these samples come from a restricted portion of the upper mantle. It is therefore probable that the nodules do not represent samples from the entire pressure interval from 10–18 kbar. If an upper mantle geotherm of ~15°/km is assumed, the depth interval sampled would be <10 km.

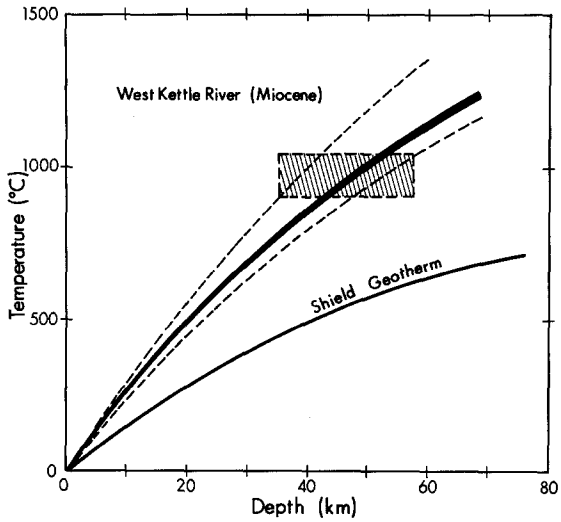

Fig. 8. Estimation of a Miocene geotherm using equilibration temperatures and depths for nodules from West Kettle River

Discussion

In this paper we have focussed principally on the green pyroxene series nodules from West Kettle River. The black pyroxene series nodules and crustal xenoliths will be discussed elsewhere. Of the green pyroxene series nodules sampled, spinel lherzolite is the dominant rock type with subordinate olivine websterite, websterite, harzburgite and dunite. This dominance of spinel lherzolite in the upper mantle beneath British Columbia has been noted previously by Littlejohn and Greenwood (1974) and by Nicholls et al. (1982).

Provided that the nodules were equilibrated in the upper mantle, the geothermal gradient in the Miocene beneath that part of British Columbia will be imprinted on the nodules. The shaded area in Fig. 8 represents the probable pressure and temperature conditions of equilibration of the West Kettle River nodules before eruption of the host basalt. Through this region has been drawn a geotherm for the Miocene with the uncertainties shown by the dashed lines. The geotherm shown in Fig. 8 is in good agreement with that obtained from heat flow measurements (Ranalli 1980). Turning this observation around, and assuming the nodules were equilibrated on Ranalli's Cordilleran geotherm (Fig. 9), the pressure of equilibration is restricted to 40–50 km depth.

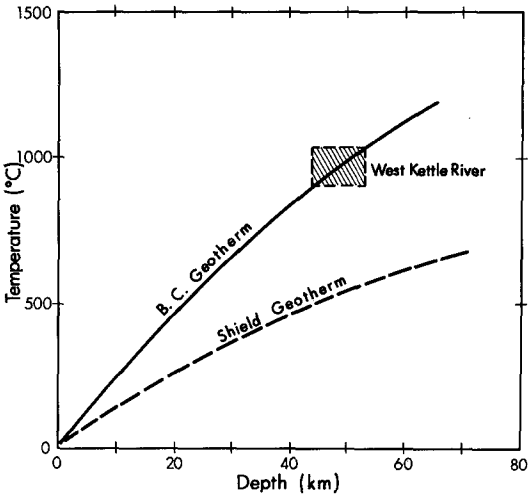

Fig. 9. Estimation of the depth of equilibration of nodules using calculated equilibration temperatures and a geotherm for the Cordillera from Ranalli (1980)

The presence of banding or layering in some nodules is strong evidence for mineralogical heterogeneities in the upper mantle beneath southern British Columbia. However, before generalizations can be made, nodules will have to be studied from other localities in southern and central British Columbia. This comparative work is now in progress (Fujii and Scarfe 1981; Brearley et al. 1982; Scarfe and Fujii, in preparation). Similar banding has been observed in nodules from other localities in North America and Australia (Irving 1980).

Some of the nodules of the green pyroxene series show melting along grain boundaries, indicating that they were heated above solidus temperatures. The estimated temperatures for the equilibration of these minerals are, however, considerably below the liquidus temperature of alkali basalt magma (e.g. Arculus 1975), indicating that the heating event was of short duration and was probably caused by the host basalt during ascent. The temperature of the magma and the residence time will determine the extent of re-equilibration of minerals within the nodules after they have been captured by the host basalt. The evidence for element migration during re-equilibration would be the preservation of chemical zoning at the margins of minerals. Because the diffusivity of cations in spinel is much greater ($\sim 10^{-9}$ cm^2/s; Halloran and Bowen 1980) than the diffusivity of cations in any of the silicate minerals (e.g. $\sim 10^{-12}$ cm^2/s in olivine; Freer 1981) in the nodules, chemical zoning is more likely to be observed in spinels. A search for such zoning in spinels, however, was unsuccessful. Using this constraint, it is possible to estimate the maximum residence time of the nodules in the host basalt prior to extrusion. The maximum residence time is given by $t \leqq x^2/D$, where x is the thickness of the chemically zoned margin and D is the diffusion coefficient of Fe^{2+} at the temperature of interest (10^{-9} cm^2/s at 1,400° C and 10^{-11} cm^2/s at 1,100° C; Halloran and Bowen 1980). The maximum suspension time will be obtained using 10^{-11} cm^2/s for D and 5 μm for x, which is a conservative estimate of the

diameter of the volume excited by the electron beam. The result is 2.5×10^4 s, or about 7 h. Finally, if it is assumed that the nodules were derived from a depth of about 50 km, the ascent rate of magma is estimated to be faster than 7 km/h. This value is in agreement with the ascent rate estimated from Stokes' law and assuming that the magma behaves as a Newtonian fluid (Spera 1979). It is not necessary, therefore, to assume non-Newtonian behaviour during magma transport.

Conclusions

Mineralogical and chemical evidence from the West Kettle River nodules, which were transported to the surface by a basanitoid melt, indicates that the upper mantle beneath southern British Columbia is dominated by spinel lherzolite, with subordinate amounts of olivine websterite, websterite, clinopyroxenite and wehrlite. Textures are typically granular and show little evidence of shear. Some of the nodules are layered with pyroxene- and olivine-rich bands. It therefore seems clear that the upper mantle beneath southern British Columbia is heterogeneous and banded on a scale of centimeters to meters. Temperatures of equilibration, which were estimated from geothermometers, are approximately 950° C at depths of 30–60 km.

Acknowledgements. We are extremely indebted to T.S. Hamilton for finding this new locality and for leading a collecting trip to the West Kettle River in the fall of 1980. Fujii acknowledges financial support from the President's Fund of the University of Alberta and Scarfe acknowledges support from NSERC Grant A8394, EMR Grant 121-4-79 and DSS contract 04SB.23254-1-0296. H.S. Yoder Jr. is thanked for permission to use the Geophysical Laboratory microprobe. Microprobe facilities at the University of Alberta are supported by funds from NSERC operating grant A4254 to D.G.W. Smith. M. Brearley, D.M. Harris, J. Nicholls and D.G.W. Smith critically reviewed the manuscript. Experimental Petrology Laboratory contribution No. 66.

References

Arculus RJ (1975) Melting behavior of two basanites in the range 10–35 kbar and the effect of TiO_2 on the olivine-diopside reactions at high pressures. Carnegie Inst Washington Yearb 74:512–515

Bence AE, Albee AL (1968) Empirical correction factors for the electron microanalysis of silicates and oxides. J Geol 76:382–403

Brearley M, Fujii T, Scarfe CM (1982) The petrology and geochemistry of ultramafic nodules from Summit Lake, near Prince George, British Columbia. Geol Assoc Can/Mineral Assoc Can Progr Abstr 7:40

Danckwerth PA, Newton RC (1978) Experimental determination of the spinel peridotite to garnet peridotite reaction in the system $MgO-Al_2O_3-SiO_2$ in the range 900–1,100° C and Al_2O_3 isopleths of enstatite in the spinel field. Contrib Mineral Petrol 66:189–201

Evans BW, Frost BR (1975) Chrome-spinel in progressive metamorphism – a preliminary analysis. Geochim Cosmochim Acta 39:959–972

Fabriès J (1979) Spinel-olivine geothermometry in peridotites from ultramafic complexes. Contrib Mineral Petrol 69:329–336

Fiesinger DW, Nicholls J (1977) Petrography and petrology of Quaternary volcanic rocks, Quesnel Lake region, east-central British Columbia. In: Baragar WRA et al. (eds) Volcanic regimes in Canada. Geol Assoc Canada Spec Pap 16:25–38

Freer R (1981) Diffusion in silicate minerals and glasses: a data digest and guide to the literature. Contrib Mineral Petrol 76:440–454

Fujii T (1976) Solubility of Al_2O_3 in enstatite coexisting with forsterite and spinel. Carnegie Inst Washington Yearb 75:566–571

Fujii T (1977) Fe–Mg partitioning between olivine and spinel. Carnegie Inst Washington Yearb 76:563–569

Fujii T, Scarfe CM (1981) Petrology of ultramafic nodules from Boss Mountain, central British Columbia. Geol Assoc Can/Mineral Assoc Can, Progr Abstr 6:A-20

Fujii T, Scarfe CM, Hamilton TS (1981) Geochemistry of ultramafic nodules from southern British Columbia: evidence for banding in the Upper Mantle. Geol Assoc Can/Mineral Assoc Can, Progr Abstr 6:A-20

Halloran JW, Bowen HK (1980) Iron diffusion in iron-aluminate spinels. J Am Ceram Soc 63:58–65

Hamilton TS (1981) Late Cenozoic alkaline volcanics of the Level Mountain Range, northwestern British Columbia: geology, petrology and paleomagnetism. Unpubl PhD Thesis, Univ Alberta, Edmonton, 490 p

Henry DT, Medaris LG (1980) Application of pyroxene and olivine-spinel geothermometers to spinel peridotites in southwestern Oregon. Am J Sci 280A:211–231

Herzberg CT (1978) Pyroxene geothermometry and geobarometry: experimental and thermodynamic evaluation of some subsolidus phase relations involving pyroxenes in the system $CaO-MgO-Al_2O_3-SiO_2$. Geochim Cosmochim Acta 41:945–957

Irving AJ (1980) Petrology and geochemistry of composite ultramafic xenoliths in alkalic basalts and implications for magmatic processes within the mantle. Am J Sci 280A:389–426

Jackson ED (1969) Chemical variation in co-existing chromite and olivine in chromite zones of the Stillwater Complex. In: Wilson HDB (ed) Magmatic ore deposits. Econ Geol Mon 4:41–71

Jackson ED, Wright TL (1970) Xenoliths in the Honolulu volcanic series, Hawaii. J Petrol 11:405–430

Kuno H, Aoki K (1970) Chemistry of ultramafic nodules and their bearing on the origin of basaltic magmas. Phys Earth Planet Inter 3:273–301

Littlejohn AL, Greenwood HJ (1974) Lherzolite nodules in basalts from British Columbia, Canada. Can J Earth Sci 11:1288–1308

Macdonald GA, Katsura T (1964) Chemical composition of Hawaiian lavas. J Petrol 5:82–133

MacGregor ID (1974) The system $MgO-Al_2O_3-SiO_2$: solubility of Al_2O_3 in enstatite for spinel and garnet peridotite compositions. Am Mineral 59:110–119

Mori T, Green DH (1978) Laboratory duplication of phase equilibria observed in natural garnet lherzolites. J Geol 86:83–97

Mori T, Banno S (1973) Petrology of peridotite and garnet clinopyroxenite of the Mt. Higasi-Akaisi Mass, Central Sikoku, Japan – subsolidus relation of anhydrous phases. Contrib Mineral Petrol 41:301–323

Nicholls J, Stout MZ, Fiesinger DW (1982) Petrologic variations in Quaternary volcanic rocks, British Columbia, and the nature of the underlying upper mantle. Contrib Mineral Petrol 79:201–218

Obata M (1976) The solubility of Al_2O_3 in orthopyroxenes in spinel and plagioclase peridotites and spinel pyroxenite. Am Mineral 61:804–816

Obata M, Banno S, Mori T (1974) The iron-magnesium partitioning between naturally occurring coexisting olivine and Ca-rich clinopyroxene: an application of the simple mixture model to olivine solid solution. Bull Soc Fr Mineral Cristallogr 97:101–107

Powell M, Powell R (1974) An olivine-clinopyroxene geothermometer. Contrib Mineral Petrol 48:249–263

Ranalli G (1980) Rheological properties of the upper mantle in Canada from olivine microrheology. Can J Earth Sci 17:1499–1505

Roeder PL, Campbell IH, Jamieson HE (1979) A re-evaluation of the olivine-spinel geothermometer. Contrib Mineral Petrol 68:325–334

Sachtleben T, Seck HA (1981) Chemical control of Al-solubility

in orthopyroxene and its implications on pyroxene geothermometry. Contrib Mineral Petrol 78:157–165
Scarfe CM, Fujii T (in preparation) Petrology and geochemistry of ultramafic nodules and their host basalts from south and central British Columbia
Sinclair PD, Templeman-Kluit DJ, Medaris LG (1978) Lherzolite nodules from a Pleistocene cinder cone in central Yukon. Can J Earth Sci 15:220–226
Smith DGW (1976) Quantitative energy dispersive microanalysis. In: Smith DGW (ed) Short course in microbeam techniques. Mineral Assoc Canada Short Course Handbook 1:63–106
Smith DGW, Gold CM (1976) EDATA2: a FORTRAN IV computer program for processing wavelength and/or energy-dispersive electron microprobe analyses. Microbeam Anal Soc Proc 14th Ann Conf (San Antonio 1979: Newbury DE ed) pp 273–278
Souther JG (1970) Volcanism and its relationship to recent crustal movements in the Canadian Cordillera. Can J Earth Sci 7:553–568
Souther JG (1977) Volcanism and tectonic environments in the Canadian cordillera – a second look. In: Baragar WRA, Coleman LC, Hall JM (eds) Volcanic regimes in Canada. Geol Assoc Canada Spec Pap 16:3–24
Spera FJ (1980) Aspects of magma transport. In: Hargraves RB (ed) Physics of Magmatic Processes. Princeton Univ Press, pp 265–323
Strong DF (1969) Formation of the hour-glass structure in augite. Mineral Mag 37:472–479
Wells PRA (1977) Pyroxene thermometry in simple and complex systems. Contrib Mineral Petrol 62:129–139
Wilshire HG, Jackson ED (1975) Problems in determining mantle geotherms from pyroxene compositions of ultramafic rocks. J Geol 83:313–329
Wilshire HG, Shervais JW (1975) Al-augite and Cr-diopside ultramafic xenoliths in basaltic rocks from western United States. In: Ahrens LH, Press F, Runcorn SK, Urey HC (eds) Physics and chemistry of the Earth. Pergamon Press 9:257–272
Wilson AD (1960) The micro-determination of ferrous iron in silicate minerals by a volumetric and a colorimetric method. Analyst 85:823–828
Wood BJ (1976) An olivine-clinopyroxene geothermometer: a discussion. Contrib Mineral Petrol 56:297–303
Wood BJ, Banno S (1973) Garnet-orthopyroxene and orthopyroxene-clinopyroxene relationships in simple and complex systems. Contrib Mineral Petrol 42:109–142
Yoder HS (1976) Generation of basaltic magma, Natl Acad Sci Washingtom, DC, 265 p

Received April 14, 1982; Accepted July 9, 1982